Metallophysics and Advanced Technologies
Металофіз. новітні технол.
Metallofiz. Noveishie Tekhnol.
2026, vol. 48, No. 9, pp. 985–998
https://doi.org/10.15407/mfint.48.09.0985
Reprints available directly from the publisher

© 2026 G. V. Kurdyumov Institute for Metal Physics,
National Academy of Sciences of Ukraine
Published by license under
the G. V. Kurdyumov Institute for Metal Physics–
N.A.S. of Ukraine Publishers imprint.
Printed in Ukraine.

PACS numbers: 68.37.Hk, 68.47.Gh, 81.05.Ni, 81.40.Cd, 81.65.Kn, 81.65.Rv, 82.45.Bb

Characteristic Features of the Selective Dissolution of the NZ30K Magnesium Alloy in Ringer–Locke Solution

V. L. Greshta[*], O. E. Narivskyi[**], A. V. Dzhus[*]

[*]*National University Zaporizhzhia Polytechnic,*
64 Zhukovskogo Str.,
UA-69063 Zaporizhzhia, Ukraine
[**]*Ukrspetsmash LLC,*
7 Haharina Str.,
UA-71100 Berdiansk, Ukraine

The paper investigates the characteristic features of the selective dissolution of the magnesium alloy NZ30K in the Ringer–Locke solution. As found, it is subjected to pitting corrosion. Metallographic analysis using a scanning electron microscopy reveals that the pitting surface has a developed relief characteristic of selective dissolution of steels and alloys. The characteristic features of the selective dissolution of alloy components in pitting are studied using the calculated coefficients of selective dissolution of zinc Z_{Zn}, zirconium Z_{Zr}, and neodymium Z_{Nd}. As believed, if these coefficients are less than one, then, the main component of the alloy, magnesium, dissolves more intensively than a specific alloying element in combination with magnesium. And, if the coefficients $Z_{Zn,\ Zr,\ Nd} > 1$, then, it is *vice versa*. As found, the intensity of selective metal dissolution on the side surface of the pitting increases in the following sequence: Zr, Mg, Nd, Zn; Zr, Nd, Mg, Zn or Mg, Zr, Nd, Zn. Under such conditions, the pitting surface is enriched with zirconium or magnesium and depleted in Mg, Nd, Zn or Zr, Nd, Zn. This contributes to the solid-phase diffusion of zirconium atoms into the alloy bulk, and magnesium, neodymium, and zinc in the opposite direction in the first case, and magnesium atoms into the alloy bulk, and Zr, Nd, and Zn in the opposite direction in the second case. As shown, the processes of solid-phase diffusion of alloy

Corresponding author: Viktor Greshta
E-mail: greshtaviktor@gmail.com

Citation: V. L. Greshta, O. E. Narivskyi, and A. V. Dzhus, Characteristic Features of the Selective Dissolution of the NZ30K Magnesium Alloy in Ringer–Locke Solution, *Metallofiz. Noveishie Tekhnol.*, **48**, No. 9: 985–998 (2026), DOI: 10.15407/mfint.48.09.0985

© Publisher PH 'Akademperiodyka' of the NAS of Ukraine, 2026. This is an open access article under the CC BY-ND license (https://creativecommons.org/licenses/by-nd/4.0)

components supports the anodic dissolution of metals in pitting, which is provided by cathodic reactions of oxygen reduction in their vicinity and hydrogen on their surface, which is formed as a result of hydration of corrosion products. As found, under such conditions, the magnesium content on the side surface of the NZ30K alloy decreases from 95.67 down to 71.84…82.57 wt.%, and it is covered with a passive film with an oxygen content from 10.02 up to 17.18 wt.%. As found, at the bottom of the pitting, the intensity of selective metal dissolution increases in the following sequence: Mg, Zn, Nd, Zr. Under such conditions, the surface of the pitting is enriched with magnesium and depleted in Zn, Nd, and Zr. This contributes to the solid-phase diffusion of magnesium atoms into the alloy bulk, and Zn, Nd, and Zr to the pitting surface. This supports the anodic processes, which are provided by cathodic hydrogen reduction reactions on their surface. As found, the oxygen content on the pitting surface decreases down to 1.92…7.8 wt.%. This shows that the passive film is denser on the side surface of the pitting than on its bottom. As proved, the pittings on the surface of the NZ30K alloy are repassivated, and, therefore, it can be considered as a material for the production of biodegradable implants.

Key words: pitting corrosion, NZ30K alloy, Ringer–Locke solution, selective dissolution of metals in NZ30K alloy pittings, biodegradable NZ30K alloy implant.

В статті досліджували характерні особливості селективного розчинення маґнійового стопу NZ30K у розчині Рінґера–Локка. Встановлено, що він піддався піттінґовій корозії. Металографічною аналізою із застосуванням растрового електронного мікроскопу встановлено, що поверхня піттінґів мала розвинутий мікрорельєф, притаманний селективному розчиненню криць і стопів. Характерні особливості селективного розчинення компонентів стопу в піттінґах досліджували, використовуючи розраховані коефіцієнти селективного розчинення цинку Z_{Zn}, цирконію Z_{Zr} і неодиму Z_{Nd}. Вважали, що, якщо ці коефіцієнти менші за одиницю, то основний компонент стопу Маґній інтенсивніше розчинявся, ніж конкретний леґувальний елемент в парі з Маґнієм. А якщо коефіцієнти $Z_{Zn,\ Zr,\ Nd} > 1$, то навпаки. Встановлено, що на бічній поверхні піттінґа інтенсивність селективного розчинення металів зростала у такій послідовності: Zr, Mg, Nd, Zn; Zr, Nd, Mg, Zn або Mg, Zr, Nd, Zn. За таких умов поверхня піттінґа збагачувалася Цирконієм або Маґнієм і збіднювалася Mg, Nd, Zn або Zr, Nd, Zn. Це сприяло твердофазній дифузії атомів Цирконію в об’єм стопу, а Маґнію, Неодиму та Цинку — в протилежному напрямку у першому випадку, та атомів Маґнію в об’єм стопу, а Zr, Nd і Zn — в протилежному напрямку в другому. Показано, що процеси твердофазної дифузії компонентів стопу підтримували анодне розчинення металів у піттінґах, яке забезпечувалося катодними реакціям відновлення Оксиґену в їхньому околі та Гідроґену на їхній поверхні, який утворювався внаслідок гідратації продуктів корозії. З’ясовано, що за таких умов вміст Маґнію на бічній поверхні стопу NZ30K понизився з 95,67 до 71,84...82,57 мас.%, і вона покрилася пасивною плівкою з вмістом Оксиґену від 10,02 до 17,18 мас. %. Встановлено, що на дні піттінґа інтенсивність селективного розчинення металів зростала у такій послідовності: Mg, Zn, Nd, Zr. За таких

умов поверхня піттінґа тут збагачувалася Маґнієм і збіднювалася Zn, Nd, Zr. Це сприяло твердофазній дифузії атомів Маґнію в об'єм стопу, а Zn, Nd і Zr — до поверхні піттінґа. Це підтримувало анодні процеси, які забезпечувалися катодними реакціями відновлення водню на їхній поверхні. Виявлено, що на поверхні піттінґа тут зменшився вміст Оксиґену до 1,92...7,8 мас.%. Це показало, що на бічній поверхні піттінґа пасивна плівка щільніша, ніж на його дні. Доведено, що піттінґи на поверхні стопу NZ30K репасивувалися, а отже, його можна розглядати як конструкційний матеріял для виробництва біорозкладних імплантів.

Ключові слова: піттінґова корозія, стоп NZ30K, розчин Рінґера–Локка, селективне розчинення металів у піттінґах на стопі NZ30K, біорозкладний імплант зі стопу NZ30K.

(Received 13 August, 2025; in final version, 12 November, 2026)

1. INTRODUCTION

Today, magnesium alloys are used to produce biodegradable implants for surgical treatment in traumatology [1]. However, they often have poor mechanical and biological properties that can be improved by various alloying methods [2–5]. In particular, Mg–Ca alloy is produced to increase bone integration with calcium, which promotes bone formation during implant biodegradation [6–8]. At the same time, it can form MgCa intermetallic inclusions, which are the focus of local corrosion, which is unacceptable in the treatment of broken bones using biodegradable implants [9–11]. At the same time, the mechanisms of these local corrosion processes remain controversial, which 'slows down' the solution of this problem and the use of these alloys in the production of biodegradable implants [12–17]. At the same time, Al–Ca-doped magnesium alloys can contribute to biological complications in fracture treatment, including muscle destruction, reduced osteoclastogenesis, and Alzheimer's disease [18]. Magnesium alloys alloyed with Zn, Zr, Nd and Ag do not have these disadvantages [19, 20]. In addition, Zn and Nd increase their strength and relative elongation, and Zr promotes grain refinement, which increases their specific shock absorption capacity and resistance to shock loads [19]. The resistance of the NZ30K alloy to the activating effect of chloride ions in the Ringer-Locke solution is provided mainly by zinc-containing oxide films on its surface, which, under certain conditions, can lead to pitting and ulcer corrosion with the formation of corrosion pores and channels under them. They are known [21, 22] to be caused by the solid-phase diffusion of atoms of the main components of steels and alloys.

Therefore, we investigated the characteristic features of the selective dissolution of NZ30K alloy in Ringer–Locke solution to substantiate the possibility of its use in the production of biodegradable im-

plants.

2. EXPERIMENTAL/THEORETICAL DETAILS

We studied samples of magnesium alloy NZ30K smelted in an induction crucible furnace and subjected to ageing [23]. The diameter of the samples was 12 and the length was 30 mm. Their chemical composition was determined by the x-ray spectral method using the JNKA ENERGY 350. The chemical composition of the studied samples is shown in Table 1.

Corrosion tests of the samples were carried out in a Ringer–Locke solution (an aqueous solution of undissociated water with the following chemical reagents, in [mg/l]: NaCl—9; $NaHCO_3$, $CaCl_2$, KCl—0.2 for each reagents; $C_6H_{12}O_6$—1) at a temperature of 20 ± 1°C. The surface of corrosion damage on the samples after their testing in Ringer–Locke's solution was examined using an optical microscope MMR-2P and a scanning electron microscope INKA ENERGY 350 with an energy dispersive microanalyser to determine the chemical composition of the alloy in local characteristic damage. The features of selective dissolution of the alloy components were evaluated by their selective dissolution coefficients Z_{Zn}, Z_{Zr}, and Z_{Nd}, which have been determined by the formula:

$$Z_{(Zn,Zr,Nd)} \frac{\Delta(Zn, Zr, Nd) \times Mg}{\Delta Mg \times C_{(Zn,Zr,Nd)}},$$

where $Z_{(Zn,\ Zr,\ Nd)}$ are the coefficients of selective dissolution of Zn, Zr and Nd, Δ(Zn, Zr, Nd) is the difference between the content of the corresponding alloying element in the alloy in the initial state and after corrosion tests in Ringer–Locke solution, wt.%; Mg—magnesium content in the alloy in the initial state, wt.% (Table 1); ΔMg is the difference between the content of Mg in the alloy in the initial state and after corrosion tests in Ringer–Locke solution, wt.%; $C_{(Zn,\ Zr,\ Nd)}$ is the content of Zn, Zr and Nd in the alloy in the initial state, wt.% (Table 1).

The chemical composition of the NZ30K alloy in pittings is presented in Table 2.

The calculated coefficients of selective dissolution of NZ30K alloy components are given in Table 3.

TABLE 1. Chemical composition of the studied samples.

Alloy	Content of chemical elements, wt.%			
NZ30K	Mg	Zn	Zr	Nd
	95.67	0.67	0.89	2.77

TABLE 2. Chemical composition of characteristic places on the surface of NZ30K alloy in pitting after corrosion tests in Ringer–Locke solution.

№	Location on the alloy surface	Content of chemical elements, wt.%				
		Mg	Zn	Zr	Nd	O
1	Fig. 2*a*, spectrum 1	78.08	1.70	0.67	0.00	17.18
		Cl = ±0.88 wt.%, Ca = 1.49 wt.%				
2	Fig. 2*b*, spectrum 3	71.84	1.40	0.87	1.57	10.02
		Cl = 13.29 wt.%				
3	Fig. 2*c*, spectrum 4	82.57	0.00	0.26	0.00	17.17
4	Fig. 3*a*, spectrum 1	90.41	0.58	0.64	5.69	2.68
5	Fig. 3*b*, spectrum 2	96.81	0.05	1.79	0.00	1.92
6	Fig. 3*c*, spectrum 3	89.00	1.00	0.00	2.20	7.80
7	Fig. 3*d*, spectrum 4	62.54	1.11	0.00	0.00	36.35

TABLE 3. Coefficients of selective dissolution of NZ30K alloy in characteristic places.

№	Local corrosion damage of the sample	Coefficients of selective dissolution of metals in local corrosion damage		
		Z_{Zn}	Z_{Zr}	Z_{Nd}
1	Fig. 2*a*, spectrum 1	8.38	0.30	5.45
2	Fig. 2*b*, spectrum 3	4.69	0.09	0.29
3	Fig. 2*c*, spectrum 4	7.33	5.19	7.33
4	Fig. 3*a*, spectrum 1	2.49	7.20	19.29
5	Fig. 3*b*, spectrum 2	73.73	80.58	79.68
6	Fig. 3*c*, spectrum 3	6.47	14.46	2.98
7	Fig. 3*d*, spectrum 4	1.90	2.89	2.89

3. RESULTS AND DISCUSSION

Previously, the corrosion behaviour of magnesium alloy NZ30K in Ringer–Locke solution has been studied in paper [5]. It has been found that it underwent pitting corrosion (Fig. 1).

On the surface of the pitting 0.5 mm to the left of spectrum 1 (Fig. 2*a*), a scanning electron microscope was used to record etched metal in the vicinity of irregularly shaped intermetallic inclusions.

This is most likely due to the increased corrosion activity of the metal on structural imperfections near inclusions in an aggressive corrosive media formed from hydrated corrosion products in pitting [24]. At the same time, as established in Refs. [25, 26], the nature, volume, and size of inclusions significantly affect the probability of metal activa-

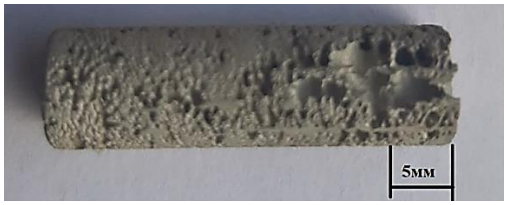


Fig. 1. Cylindrical surface of the NZ30K alloy sample subjected to pitting corrosion in Ringer–Locke solution.

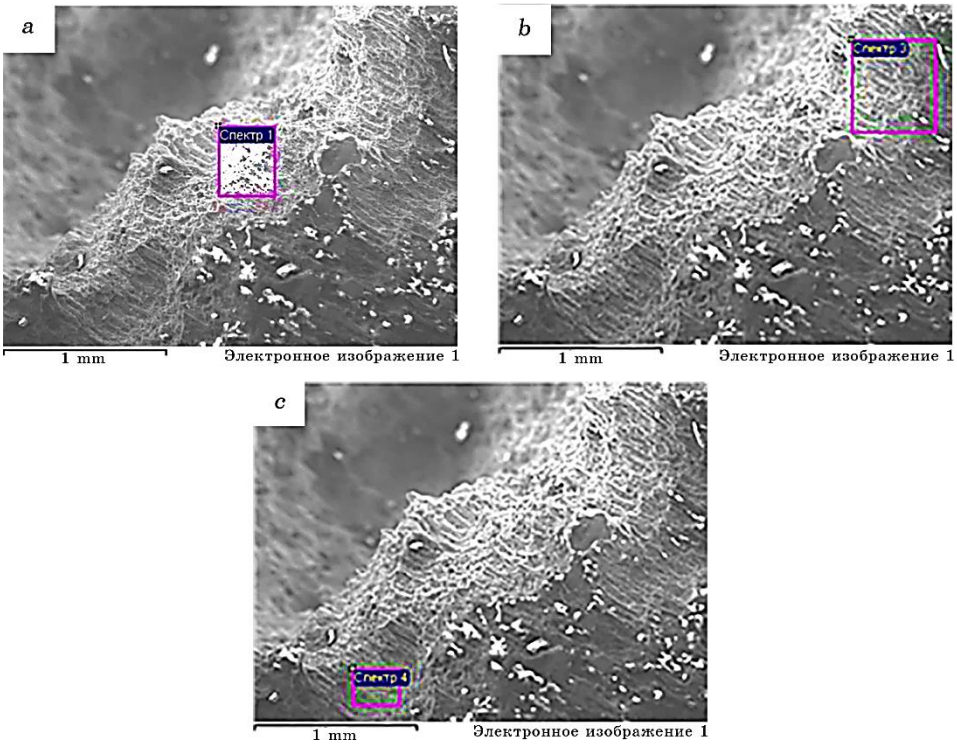


Fig. 2. Pitting surface on a sample of NZ30K alloy after testing in Ringer–Locke solution: *a*—spectrum 1, *b*—spectrum 3, *c*—spectrum 4.

tion in their vicinity, which is characterized by the peculiarities of selective alloy dissolution.

The selective nature of the alloy dissolution in pitting is confirmed by the developed microrelief of its surface, which was recorded using a scanning electron microscope (Figs. 2, 3) and the results of the analysis of the calculated coefficients of selective dissolution of $Z_{Zn,\ Zr,\ Nd}$ metals on their surface (Table 3).

In particular, from the analysis of item 1 of Table 3, it has been

found that the coefficients of selective dissolution of Zn (Z_{Zn}= 8.38) and Nd (Z_{Nd} = 5.45) are greater than one. This indicates that, in this area of the pitting (Fig. 2*a*), Zn and Nd dissolved more intensively than Mg.

Under such conditions, its surface was enriched in Mg and depleted in Zn and Nd. At the same time, it has been calculated that the coefficient Z_{Zr} <1, which indicates a more intense dissolution of Mg than Zr. This led to the fact that the pitting surface (Fig. 2*a*) was enriched in Zr and depleted in Mg. In general, it should be noted that according to the data in item 1 of Table 3, the intensity of metal dissolution in this area of the pitting increased in the following order: Zr, Mg, Nd, Zn. This tendency was supported by the solid-phase diffusion of Mg, Nd, and Zn atoms in the alloy volume to the pitting surface, and Zr in the opposite direction. The solid-phase diffusion of Mg atoms, which is the main component of the alloy, to the surface of the pitting can cause the formation of corrosion pores, channels, *etc.* under their surface. It is known [27] that the ionization of a chemical element with a negative

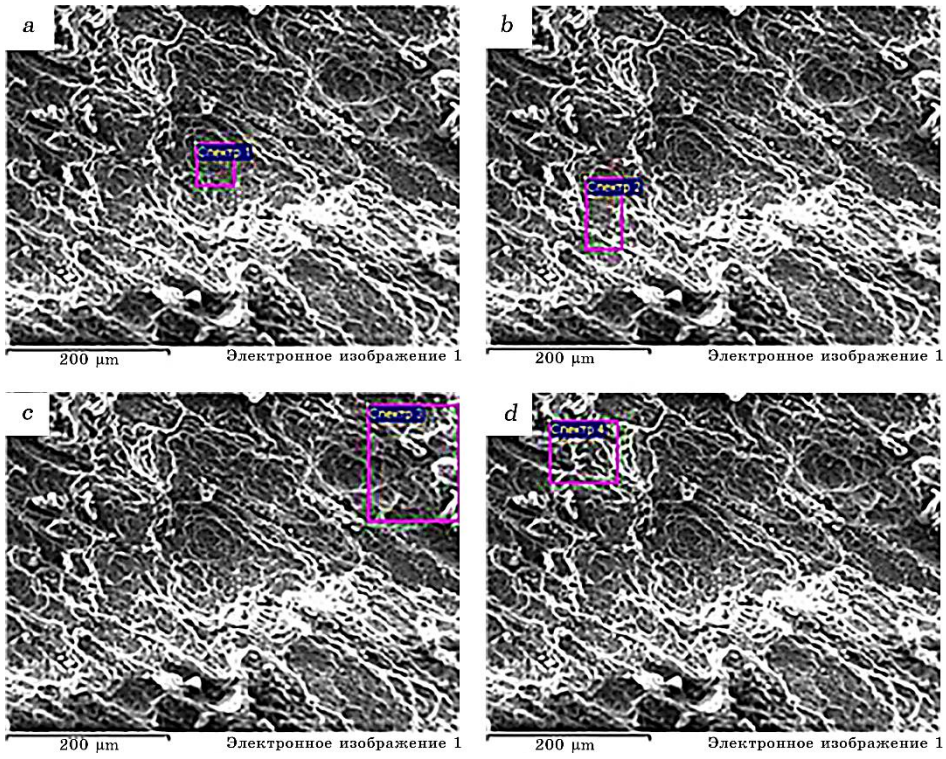


Fig. 3. Microphotography of the bottom of the pitting on the surface of the NZ30K alloy sample after testing in Ringer–Locke solution: *a*—spectrum 1; *b*—spectrum 2; *c*—spectrum 3; *d*—spectrum 4.

electrode potential on the alloy surface promotes the formation of nonequilibrium vacancies that diffuse into the alloy volume, where they coagulate and form pores. Such defects in the structure of the NZ30K alloy, alloyed with silver and clad with a layer of silver, were recorded by the authors of Ref. [20] in pitting. However, no microstructural defects associated with the solid-phase diffusion of atoms of its components in the vicinity of the pittings were observed in the pittings on the surface of the alloy under study (Figs. 2, 3). This is most likely due to the fact that the solid-phase diffusion of Mg atoms, which is the main component of the NZ30K alloy, is much slower than that of Zn and Nd atoms. At the same time, the counter-solid-phase diffusion of atoms of these chemical elements and oxygen to the pitting surface contributes to the formation of a passive film of Zn oxides. Indeed, here (Fig. 2*a*, spectrum 1), the zinc content increased to up 1.7 and oxygen up to 17.18 wt. Zinc, like chromium, is a 'valve' metal, which means that it forms passive films with semiconducting properties. The pitting resistance of steels and alloys depends on the properties of passive films [28]. It is characterized by the pitting potential [29, 30] or critical pitting temperatures [21, 22], which depend on the temperature of chloride-containing media, pH, chloride concentration, *etc.* [25, 31, 32]. At the same time, studies [21, 22, 25, 26] have established that the protective properties of passive films on the surface of passivated steels and alloys depend on the content of chromium, which is a 'valve' metal.

Most likely, the Zn content in NZ30K alloy also affects the characteristics of the passive film on its surface, which consists of Zn, Zr, and Nd oxides. Obviously, the content of these oxides in the passive film depends on the characteristics of the selective dissolution of the components of this magnesium alloy. In particular, on the surface of the pitting (Fig. 2*a*), the content of zinc oxides is maximum, and zirconium is minimal (see item 1, Table 3). The same trend was found in place (Fig. 2*b*). However, the analysis of the coefficients of selective dissolution Z_{Zn}, Z_{Zr}, and Z_{Nd} (item 2 of Table 3) revealed that Mg dissolved much more intensively from the alloy surface than Zr and Nd. After all, their selective dissolution coefficients are much less than one. It should be noted that the passive film on this alloy surface consisted mainly of Zn oxides, since the coefficient $Z_{Zn} >> 1$. Under such conditions, zinc dissolved more intensively than magnesium, and the counter-solid-phase diffusion of its atoms and oxygen on the pitting surface contributed to the formation of a passive film of zinc oxides with a slightly lower oxygen content (up to 10.02 wt.%, item 2 of Table 2). In general, from the analysis of the coefficients Z_{Zn}, Z_{Zr}, and Z_{Nd} (item 2 of Table 3), it turns out that the intensity of selective dissolution of metal atoms in the pitting (Fig. 2*b*) increased in the following order: Zr, Nd, Mg, Zn. Thus, it turns out that its surface was enriched in Zr and de-

pleted in Nd, Mg, and Zn. This contributed to the solid-phase diffusion of Zr atoms into the volume of alloy on the surface of the pitting, and Nd, Mg, and Zn atoms in the opposite direction. This nature of solid-phase diffusion usually contributes to the formation of corrosion pores, channels and tunnels, *etc.* [5, 20, 27]. After all, the dissolution of solid solutions with a high content of a component with a negative electrode potential is accompanied by surface reorganization due to solid-phase diffusion. (Standard electrode potentials: Mg = –2.37; Zn = –0.763; Zr = –1.45; Nd = –2.443 V). However, they were not found here (Fig. 2*b*). This may be due to the fact that only at potentials that exceed the critical ones, reorganization of surface layers with the formation of the above-mentioned structural defects is observed [33–35]. Such a condition for the formation of corrosion pores due to the solid-phase diffusion of the main component of the Mg alloy to the surface of the pitting is more important than the nature of the selective dissolution of metals in them. Indeed, these structural defects were not found on the studied areas of the pitting surface (Fig. 2). It should be noted that a common feature for the studied pitting areas is more intense dissolution of magnesium than zinc. Under such conditions, its surface is covered with a zinc-containing dense oxide film, which is indirectly confirmed by the consistently high oxygen content in these pitting areas (Fig. 2). This correlates with the coefficients of selective dissolution Z_{Zn} and Z_{Nd}, which are much greater than one (Fig. 2*a*, *c*) and their value in place (Fig. 2*b*) (items 1–3 of Table 2). At the same time, it should be noted that at the base of the pitting (Fig. 2*c*), its surface was rapidly repassivated, since a passive film of complex oxides of Zn, Zr, and Nd on it has been formed. This is evidenced by the coefficients Z_{Zn}, Z_{Zr}, and Z_{Nd}, which are much greater than one (item 3 of Table 3). From their analysis, it follows that the alloying elements of the alloy in the pitting were selectively dissolved in the following series: Mg, Zn, Zr, Nd. This process was supported by the solid-phase diffusion of magnesium atoms into the alloy volume, and Zn, Zr, and Nd in the opposite direction. It is known [5, 20] that such a character of solid-phase diffusion of magnesium atoms in the vicinity of pitting does not lead to the formation of the above-mentioned defects in the structure of the NZ30K alloy. At the same time, a general trend should be noted, in particular, the more intense the selective dissolution of Zn, Zr, and Nd on the pitting surface (Fig. 2) (items 1–3, Table 3), the lower the corrosion loss of magnesium in them (items 1–3, Table 2). This makes it impossible to form corrosion pores, channels, *etc.*

The selective dissolution of magnesium in pitting on the surface of NZ30K alloy in Ringer–Locke solution proceeded in stages in pairs Mg–Zn, Mg–Zr, and Mg–Nd and depended on the intensity of neodymium dissolution relative to magnesium. It has been found that the higher the value of the coefficient Z_{Nd}, the lower the corrosion loss of

Mg on the pitting surface (items 1–3 of Tables 2, 3). This is due to the fact that the standard electrode potential of Nd (–2.443 V) is more negative than that of Mg (–2.37 V). According to Refs. [27, 36–38], this is due to the fact that the less thermodynamically stable Nd dissolved selectively, accelerating the dissolution of magnesium.

The analysis of the microphotography of the bottom of the pitting (Fig. 3) showed that its surface has a developed character inherent in the selective dissolution of metals. The peculiarities of selective dissolution of the alloy are associated with the thermodynamic properties of the set of metal atoms that are in their composition [33, 39].

This is consistent with the information presented in [30, 40], since it was found that corrosion losses of steel type 18-10 decrease, and those of alloy 23–28 increase with an increase in their specific paramagnetic susceptibility χ_0. This tendency is explained by the Tammann's limit conditions, which are determined, as mentioned in [33, 39], by the thermodynamic properties of the set of metal atoms in the alloy. That is why, at the bottom of the pitting in the presence of an acidic corrosive media [41–44], more intensive dissolution of alloying elements than the main component of the NZ30K magnesium alloy has been found. Indeed, the coefficients of selective dissolution Z_{Zn} varied from 1.9 (Fig. 3.2, item 7 of Table 3) up to 73.73 (Fig. 3*b*, item 5 Table 3), Z_{Zr} from 2.89 (Fig. 3*d*, item 7 of Table 3) to 80.58 (Fig. 3*b*, item 5 of Table 3), Z_{Nd} from 2.89 (Fig. 3*d*, item 7 of Table 3) up to 79.68 (Fig. 3*b*, item 5 of Table 3). Under such conditions, the surface of the pitting bottom was mainly enriched with magnesium (Fig. 3*a*, *b*; items 4, 5 of Table 2), but it was depleted in oxygen down to 2.68 and 1.92 wt.% (items 4, 5 of Table 2). At the same time, it should be noted that the lateral surface of the pitting (Fig. 2*a*–*c*, items 1–3 of Table 2) is much more depleted in Mg than the surface at its bottom (Fig. 3*a*–*c*, items 4–6 of Table 2). This is most likely due to the lower access of oxygen to it (see items 1–6 of Table 2), which made cathodic depolarization by oxygen impossible and reduced the anodic processes of metal dissolution in the pitting, which were supported almost exclusively by cathodic processes with hydrogen depolarization. It should be noted that the anodic processes of metal dissolution in the pitting (Fig. 3), even in a small area of 500×500 μm, proceeded with different intensities. Indeed, from the analysis of the coefficients of selective dissolution of Zn, Zr, and Nd in the pitting (Fig. 3, items 4–7 of Table 3), it turns out that in the area (Fig. 3*a*) the intensity of metal dissolution in the pitting increased in the following sequence: Mg, Zn, Zr, Nd. Almost the same trend was recorded at the points (Fig. 3*b*, *d*), but at the point (Fig. 3*c*) the intensity of metal dissolution in the pitting increased in the following order: Mg, Nd, Zn, Zr. Thus, summarizing the above, it can be noted that on the entire surface at the bottom of the pitting, magnesium dissolved the slowest, which is typical for metastable pittings that are repassiv-

ated [45], and Nd and Zr mostly dissolved the most intensively. This, taking into account the information from [33, 39], could contribute to the slowdown of selective dissolution of zinc in the Mg–Zn pair and the formation of a zinc-containing oxide film on the pitting surface and its repassivation. It should be noted that at the location of spectrum 4 (Fig. 3*d*), the lowest magnesium content (62.54 wt.%) and the highest oxygen content (36.35 wt.%) were found on the pitting surface (item 7 of Table 2), which is associated with the accumulation of corrosion products here, but this did not affect the overall nature of the selective dissolution of metals.

Summarizing the above-mentioned, it can be noted that the NZ30K alloy dissolved selectively in the pitting formed during the testing of the sample in the Ringer–Locke solution. The most intense dissolution of magnesium on the side surfaces of the pitting has been recorded. This is due to the fact that here the anodic processes of selective dissolution of metals were supported by cathodic reactions of oxygen dissolved in the solution and hydrogen formed as a result of hydration of corrosion products. At the bottom of the pitting, anodic dissolution of metals was supported only by cathodic reactions of hydrogen reduction. Under such conditions, much less oxidation of the pitting surface was recorded with the formation of a passive film, which mainly consisted of zinc oxides. It has been found that the intensity of metal dissolution in the pitting increased in the following sequence: Mg, Zn, Nd, Zr. This process was supported by the solid-phase diffusion of magnesium atoms into the alloy volume, and Zn, Nd, and Zr in the opposite direction. This nature of solid-phase diffusion of the atoms of the main component of the alloy did not contribute to the formation of corrosion pores and channels, which makes it possible to consider the NZ30K alloy as a material for the production of biodegradable implants.

4. CONCLUSION

The results of corrosion tests of NZ30K alloy samples in a chloride-containing Ringer–Locke solution showed that they were subjected to pitting corrosion. It has been found that the alloy components dissolved selectively in the pitting. Energy dispersive analysis of the alloy surfaces showed that the intensity of selective dissolution of metals on the side surface of the pitting increased in the following sequence: Mg, Zr, Nd, Zn or Zr, Mg, Nd, Zn and Zr, Nd, Mg, Zn. These processes were supported by the solid-phase diffusion of zirconium atoms into the alloy volume and magnesium, neodymium, and zinc in the opposite direction, or magnesium atoms into the alloy volume and Zr, Nd, and Zn to the pitting surface. Under such conditions, a decrease in the magnesium content on the pitting surface from 95.67 down to 71.84…82.57

wt.% and its oxidation with an oxygen content of 10.02 to 17.18 wt.%. This is due to the fact that anodic processes were supported by cathodic reactions of hydrogen and oxygen reduction. It has been found that the intensity of selective dissolution of metals on the surface of the pitting bottom mainly increased in the following order: Mg, Zn, Nd, Zr. These processes were supported by the solid-phase diffusion of magnesium atoms into the alloy volume, and Zn, Nd, Zr in the opposite direction. Under such conditions, we recorded lower corrosion losses of magnesium at the bottom of the pitting (Mg content: 89.00…90.48 wt.%) than on its lateral surface and a lower degree of its oxidation (oxygen content from 1.92 to 7.8 wt.%). This is due to the fact that here the anodic processes were supported only by cathodic reactions of hydrogen reduction. Analysis of the characteristics of the selective dissolution of metals in pitting showed that they were repassivated without the formation of corrosion pores and channels, which makes it possible to consider this alloy for the production of biodegradable implants.

AUTHORS' CONTRIBUTIONS

V. L. Greshta conceived and designed the study, planned and coordinated the corrosion tests, analysed the experimental data on selective dissolution and pitting behaviour of NZ30K alloy, interpreted the results in the context of biodegradable implant applications, and wrote the main part of the manuscript. O. E. Narivskyi provided expert consultancy as a corrosion specialist, advised on the choice of testing conditions and electrochemical interpretation of pitting and selective dissolution processes, contributed to the discussion of the results with reference to current corrosion theories and literature, and critically revised the manuscript for important intellectual content. A. V. Dzhus, participated in the organisation and partial performance of corrosion experiments and microstructural/EDS studies, processed and systematized the experimental data (including Tables 1–3 and the analysis of pits morphology), contributed to the literature review and drafting individual sections of the text, and was responsible for the technical preparation and formatting of the manuscript according to the journal requirements.

All authors discussed the results, contributed to the final interpretation, and approved the final version of the manuscript.

REFERENCES

1. H. Li, Y. Zheng, and L. Qin, *Prog. Nat. Sci.-Mater. Int.*, **24**, Iss. 5: 414 (2014).
2. R.-C. Zeng, L. Sun, Y. F. Zheng, H. Z. Cui, and E.-H. Han, *Corros. Sci.*, **79**: 69 (2014).
3. R.-C. Zeng, S. Ii, L.-Y. Cui, X.-T. Li, E.-H. Han, and L. Song, *Front. Mater.*

Sci., **11**: 284 (2017).
4. Y. F. Zheng, X. N. Cu, and F. Witte, *Mater. Sci. Eng.-R-Rep.*, **77**: 1 (2014).
5. V. Greshta, O. Narivskyi, and A. Dzhus, *Eurasian Phys. Tech. J.*, **21**, Iss. 3: 6 (2024).
6. T. C. Lowe and R. Z. Valiev, *Adv. Biomater. Biodevices (Wiley Blackwell)*, p. 1 (2014).
7. J. W. Seong and W. J. Kim, *Corros. Sci.*, **98**: 372 (2015).
8. Z. Li, X. Gu, S. Lou, and Y. Zheng, *Biomaterials*, **29**, Iss. 10: 1329 (2008).
9. F. Cao, Z. Shi, G.-L. Song, M. Lui, and A. Atrens, *Corros. Sci.*, **79**: 69 (2013).
10. K. Gusieva, C. H. J. Davies, J. R. Scully, and N. Birbilis, *Int. Mater. Rev.*, **60**: 169 (2015).
11. W.-C. Kim, J.-G. Kim, J.-Y. Lee, and H.-K. Seok, *Mater. Lett.*, **62**, Iss. 25: 4146 (2008).
12. Y. Jin, C. Blawert, F. Feyerabend, J. Bohlen, M. del R. Silva Campos, S. Gavras, B. Wiese, D. Mei, M. Deng, H. Yang, and R. Willumeit, *Corros. Sci.*, **158**: 108096 (2019).
13. E. K. Brooks and M. T. Ehrensberger, *J. Funct. Biomater.*, **8**, Iss. 3: 38 (2017).
14. M. Esmaily, J. E. Svensson, S. Fajardo, N. Birbilis, G. S. Frankel, S. Virtanen, R. Arrabal, S. Thomas, and L. G. Johansson, *Prog. Mater. Sci.*, **89**: 192 (2017).
15. A. D. King, N. Birbilis, and J. R. Scully, *Electrochim. Acta*, **121**: 394 (2014).
16. M. Curioni, F. Scenini, T. Monetta, and F. Belucci, *Electrochim. Acta*, **166**: 372 (2015).
17. Y. Gao, A. Yerokhin, E. Parfenov, and A. Mathews, *Electrochim. Acta*, **149**: 218 (2014).
18. P. C. Ferreira, K. D. A. Piai, A. M. M. Takayanagui, and S. I. Segura-Mucoz, *Rev. Latino-Am. Enfermagem*, **16**, Iss. 1: 151 (2008).
19. M. D. Lastra, R. Pastelin, A. Camacho, B. Monroy, and A. E. Aguilar, *J. Trace Elem. Med. Biol.*, **15**, No. 1: 5 (2001).
20. V. Greshta, O. Narivskyi, A. Dzhus, V. Vynar, and O. Kuprin, *Int. Multidiscip. Sci. GeoConf. SGEM*, **24**, Iss. 6.1: 41 (2024).
21. O. E. Narivskyi, S. O. Subbotin, T. V. Pulina, S. O. Leoshchenko, M. S. Khoma, and N. B. Ratska, *Mater. Sci.*, **58**, Iss. 5: 1 (2023).
22. O. E. Narivskyi, S. O. Subbotin, T. V. Pulina, S. O. Leoshchenko, M. S. Khoma, and N. B. Ratska, *Mater. Sci.*, **59**, Iss. 5: 275 (2024).
23. V. L. Greshta, V. A. Shalomeev, A. V. Dzhus, and O. A. Mityaev, *New Mater. Technol. Metall. Eng.*, **2023**, Iss. 2: 14 (2023).
24. O. E. Narivs'kyi, *Fiz.-Khim. Mech. Mater.*, **41**, Iss. 1: 104 (2005).
25. O. E. Narivskyi, S. O. Subbotin, and T. V. Pulina, *Phys. Sci. Technol.*, **10**, Iss. 3–4: 48 (2023).
26. A. V. Dzhus, O. E. Narivskyi, S. A. Subbotin, T. V. Pulina, G. V. Snighnoi, and S. D. Leoshchenko, *Metallofiz. Noveishie Tekhnol.*, **46**, No. 4: 371 (2024).
27. J. O. Fritz and H. W. Pickering, *J. Electrochem. Soc.*, **138**, Iss. 11: 3209 (1991).
28. L. Martinez, B. Malki, G. Berthome, B. Baroux, and F. Perez, *Surf. Coat. Technol.*, **201**: 1671 (2006).
29. C. Alonso, M. Castellote, and C. Andrade, *Electrochim. Acta*, **47**: 3469 (2002).
30. O. E. Narivs'kyi, G. V. Snizhnoi, T. V. Pulina, V. L. Snizhnoi, and N. A. Solidor, *Mater. Sci.*, **59**, Iss. 3: 649 (2024).
31. G. Wranglen, *Mater. Sci. Appl.*, **6**, Iss. 4: 62 (2015).
32. Q. Zhang, R. Wang, M. Kato, and K. Nakasa, *Scripta Mater.*, **52**: 227 (2005).

33. V. V. Losev and A. P. Pchelnikov, *Results of Sci. Technol. Electrochemistry*, **15**: 62 (1979) (in Russian).
34. T. P. Moffat, F.-R. F. Fan, and A. J. Bord, *J. Electrochem. Soc.*, **138**, No. 11: 3224 (1991).
35. N. D. Tomashov, *Teoriya Korrozii i Zashchita Metallov* [Corrosion Theory and Protection of Metals] (Moskva: AN USSR: 1959) (in Russian).
36. I. D. Zartsyn, A. E. Shugurov, and I. K. Marshakov, *Zashchita Metallov*, **33**, No. 5: 453 (1997) (in Russian).
37. A. V. Plaskaev and V. M. Knizheva, *Proc. 12th Perm Conf. Corros. Prot. Metals* (1990).
38. M. Pourbaix, *Atlas of Electrochemical Equilibrium in Aqueous Solutions* (Oxford: Pergamon Press: 1974).
39. N. V. Vyazovikina, *Electrochemistry*, **28**, No. 6: 917 (1992).
40. A. V. Dzhus, O. E. Narivskyi, G. V. Snizhnoi, T. V. Pulina, and V. L. Snizhnoi, *Metallofiz. Noveishie Tekhnol.*, **46**, No. 8: 739 (2024).
41. A. Narivskiy, G. Yar-Mukhamedova, E. Temirgaliyeva, M. Mukhtarova, and Y. Yar-Mukhamedov, *Int. Multidiscip. Sci. GeoConf. SGEM*, **1**: 63 (2016).
42. E. G. Wenn and R. C. Alkire, *J. Electrochem. Soc.*, **149**: 280 (2002).
43. H. Krawiec, V. Vignal, O. Heintz, and R. Altra, *Electrochim. Acta*, **51**, Iss. 16: 3235 (2006).
44. G. Lang, M. Ujvari, and G. Horanyi, *Corros. Sci.*, **45**, Iss. 1: 1 (2003).
45. O. Narivs'kyi, R. Atchibayev, A. Kemelzhanova, G. Yar-Mukhamedova, G. Snizhnoi, and S. Subbotin, *Eurasian Chem.-Technol. J.*, **24**, No. 4: 295 (2022).